

EXTENSIVE AIR SHOWERS IN HANOI

PHAM NGOC DIEP, PHAM NGOC DONG, PHAM THI TUYET NHUNG,
PIERRE DARRIULAT, NGUYEN THI THAO
DANG QUANG THIEU AND VO VAN THUAN
VATLY, Institute for Nuclear Science and Technology,

Abstract. A set of four Cherenkov counters is currently operated on the roof of VATLY, a cosmic ray laboratory located in Ha Noi. Three of these are used to provide a trigger on extensive air showers to which the response of the fourth main counter can be studied in an unbiased way. The triple coincidence rate is of the order of 0.1 Hz. The showers selected are shown to be nearly vertical and to have energies in the range of a few hundred GeV with a core density on ground of the order of 1 m^{-2} . The response of the main counter to such showers is briefly discussed.

I. INTRODUCTION

VATLY is a cosmic ray laboratory located in Ha Noi and operated in close association with the Pierre Auger Observatory (PAO) in Argentina [1]. In addition to contributions to the analysis of PAO data, VATLY performs measurements of its own, using detectors installed on the roof of the laboratory [2]. Among these is a replica of a PAO water Cherenkov counter used to gain direct experience of its response to particles of different kinds. In particular, its response to atmospheric muons has been shown to be essentially proportional to their track length in the water volume. At the same time, it has revealed an insufficient optical quality resulting in a light loss by a factor of the order of 4 with respect to PAO counters. Accordingly, a complete refurbishing of the VATLY counter has been made, including new wall coating, improved water filtering and photomultiplier tubes (PMT's) of a better quality. In addition, three smaller counters have been constructed and installed around the main counter in order to provide a trigger on extensive air showers. The idea is that a triple coincidence of these smaller counters should select showers having a large particle density in the main counter and therefore allow for a detailed and unbiased study of its response to air showers. The operation of these smaller trigger counters and the study of the air showers on which they trigger are the subject of the present article. The paper is organized in four parts: description of the apparatus, data reduction and analysis, interpretation in terms of a simple model and response of the main counter.

II. DESCRIPTION OF THE APPARATUS

A plan view of the set of VATLY Cherenkov counters is shown in Fig. 1. The main counter, with a volume of 12,000 litres of water, cannot be moved. The three smaller counters, used as a trigger, had to be installed around it within the constraints inherent to the environment: limited roof size and limited time acceptance of the electronics allowing

for delays between tanks not exceeding 50ns – or equivalently 15 m. Moreover the cost had to be kept low. These constraints governed the design of the detector. In particular, relatively modest optical quality was considered sufficient as long as the trigger threshold of each tank could be kept low enough to allow for a triple coincidence rate in the 0.1 Hz range allowing for the collection of some 50,000 events a week.

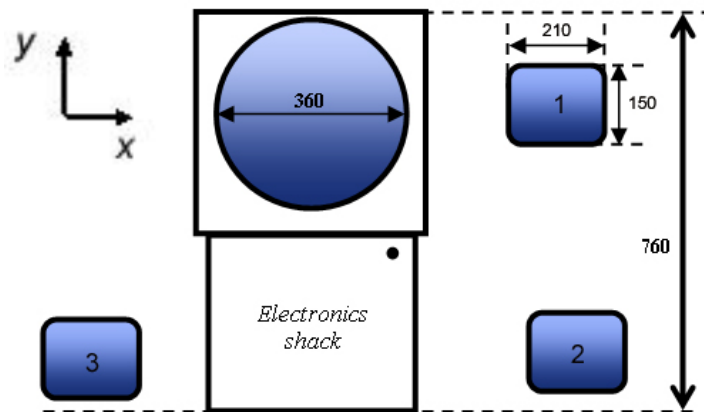


Fig. 1. Plan view of the VATLY Cherenkov counters including three small (3,000 l) tanks used as a trigger and a large (12,000 l) main tank. All distances are measured in centimetres. The black dot in the electronics shack shows the hole through which the signal and high voltage cables reach the counting room.

The small tanks are standard 3,000 l cylindrical stainless steel containers, 1.5 m in diameter and 2.1 m long, equipped with two top holes where 8" PMT's are installed. The inner walls are kept raw, without any coating, and the radiator is water from the city supply that had been filtered and kept for two years in the main tank, allowing for dust to settle. The PMT photocathodes are in direct contact with water (Fig. 2), and therefore grounded. Accordingly, the PMT anodes are at high voltage and their signals are read through a capacitor. In practice, two PMT's are supplied with a same high voltage in order to save equipment. The high voltage and signal cables, each 10 m long, reach the data acquisition electronics through a hole in the roof.

The data acquisition electronics includes the trigger logic, using NIM standard, and the data acquisition proper, using CAMAC standard. A simplified electronics diagram is shown in Fig. 3. The trigger is an OR of the three possible double tank coincidences, the requirement of a triple coincidence being kept for the off line analysis. Each of the six PMT signals is amplified by a factor of 10 before being passively split in two parts: one feeds analog-to-digital converters (ADC's) measuring the signal charges (0.25 pC/channel) and the other feeds discriminators; the discriminator outputs, 40 ns wide, serve as inputs to the trigger electronics and stop time-to-digital converters (TDC's) having a resolution of 0.2 ns/channel. The trigger provides the 160 ns wide gate to the ADC's and the start signal to the TDC's; at the same time it starts the data conversion process in the CAMAC units. A 10 kHz clock feeds a scaler used to measure the time between successive triggers

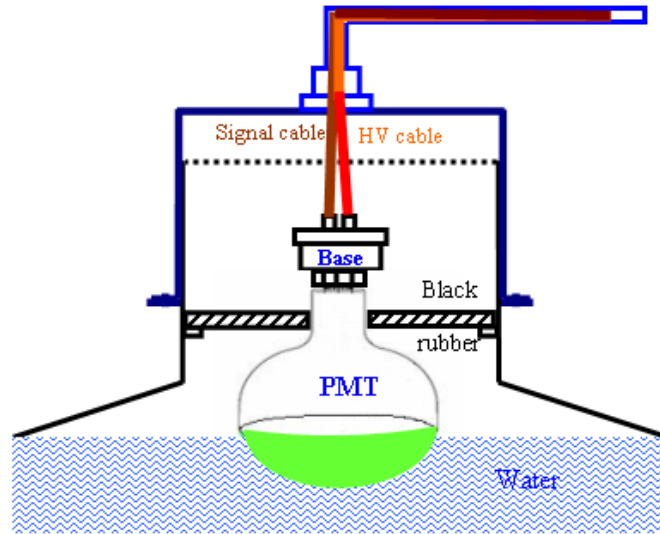


Fig. 2. Schematic PMT arrangement in the small Cherenkov tanks.

and a short dead time is generated to prevent new triggers to occur before the end of the conversion process.

III. DATA REDUCTION AND ANALYSIS

In the first step, the ADC data are pedestal subtracted. This takes advantage of the fact that the trigger requires only double tank coincidences: most triggers include an empty tank for which the pedestals can be monitored. In the second step, the PMT signals are normalized to a common mean value: this is necessary because the constraint of having two PMT's fed by a same high voltage supply prevents their gains to be fine tuned. The low light level and the tank geometry are such that the correlation between the charges collected by the two PMT's of a same tank is weak: a measurement uncertainty on the tank charges of the order of 35% has been evaluated from the data. The distribution of the sum of the tank charges (for tanks contributing to the triple coincidence trigger) is shown in Fig. 4.

The TDC data of triple coincidence events illustrate the proper operation of the electronics (Fig. 5a to 5e). One of the six PMT's is easily recognized as having defined the timing of the trigger (used as TDC start) because its TDC signal falls on the spike of the distribution. Its partners (one in the same tank and two in the other tank of the tank pair defining the trigger timing) are seen to arrive earlier while in the third tank at least one PMT signal is seen to arrive later, the other being unconstrained. These results are in agreement with expectation as the timing of a coincidence is defined by the latest of the input signals and the timing of an OR by the earliest of the input signals. As in the case of the ADC signals, mostly because of time slewing and geometry effects, the correlation between the timings of the two PMT's of a same tank is weak. The distributions of

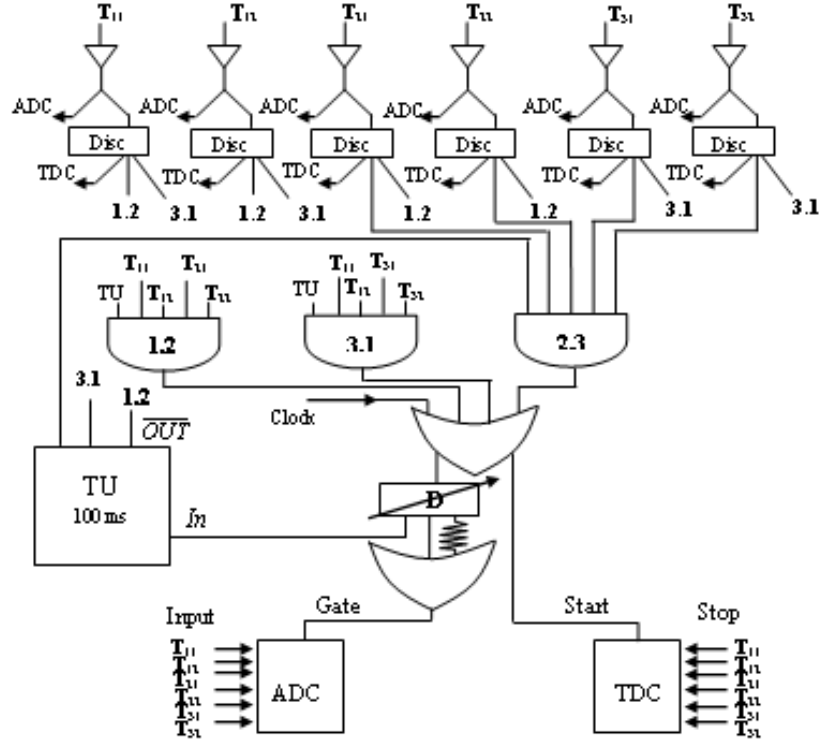


Fig. 3. Electronics diagram of the trigger logic.

their differences (Fig. 5f) have rms values of 12 ns. To a good approximation, neglecting correlations, we expect the uncertainties on the tank time, defined as the arithmetic mean of the PMT's times, to be half this value, namely 6 ns.

The distributions of the time elapsed between successive triggers and between successive triple coincidences, as measured from the 10 kHz clock, are exponentials corresponding to rates of 0.54 and 0.098 Hz respectively, in good agreement with the corresponding numbers of events collected during the 45 hours live time of the measurement.

Triple coincidences allow for reconstructing the direction of the shower axis. As shown in Fig. 6 the tank time t_i (average of the two PMT times) measured in tank i and its distance ρ_i to the shower axis obey the relations:

$$\rho_i^2 = -t_i^2 + (x_{imp} - x_i)^2 + (y_{imp} - y_i)^2 + (z_{imp} - z_i)^2 \quad (1)$$

$$t_i = (x_{imp} - x_i)\sin\theta\cos\varphi + (y_{imp} - y_i)\sin\theta\sin\varphi + (z_{imp} - z_i)\cos\theta \quad (2)$$

where θ and φ are the zenith angle and respectively azimuth of the shower axis, $x, y, z|_i$ the coordinates of the tank centres and $x, y, z|_{imp}$ those of the impact point of the shower axis on the roof of the laboratory. The quantities $\alpha = \sin\theta\cos\varphi$ and $\beta = \sin\theta\sin\varphi$ are obtained from the t_i using the relations:

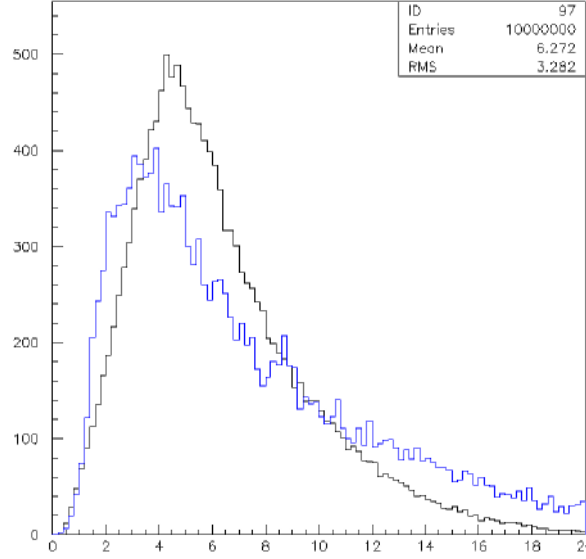


Fig. 4. Distribution of the charge collected in the PMTs of the small tanks (averaged over the two PMTs of each tank and summed over the three tanks). The narrower histogram is the prediction of the model when assigning 45 ADC channels to each “particle”.

$$\alpha = \frac{D(t, y)}{D(x, y)} \quad \text{and} \quad \beta = \frac{D(t, x)}{D(x, y)} \quad (3)$$

with

$$D(a, b) = a_1(b_2 - b_3) + a_2(b_3 - b_1) + a_3(b_1 - b_2). \quad (4)$$

In the present geometry, where x_1 and x_2 on one hand, y_2 and y_3 on the other are nearly equal, Relations 3 and 4 reduce, to a good approximation, to

$$\alpha = \frac{t_3 - t_2}{x_3 - x_2} \quad \text{and} \quad \beta = \frac{t_1 - t_2}{y_2 - y_1} \quad (5)$$

Moreover, as $(y_2 - y_1)$ is twice as small as $(x_3 - x_2)$, the uncertainty $\Delta\beta$ attached to the measurement of β is twice as large as the uncertainty $\Delta\alpha$ attached to the measurement of α .

To the extent that the φ distribution is uniform, a good approximation in the present case, we expect the relation $Rms(\alpha)^2 - Rms(\beta)^2 = \Delta\alpha^2 - \Delta\beta^2$ to be obeyed by the rms values of the α and β distributions independently from the zenith angle distribution. This relation provides a measurement of the uncertainties on the tank times in perfect agreement with the earlier independent estimate of 6 ns.

It is some time convenient to consider data samples associated with different thresholds applied to the PMT charges. In practice we used thresholds of 2, 10 and 18 ADC channels, the former being just above discriminator threshold and giving a three tank

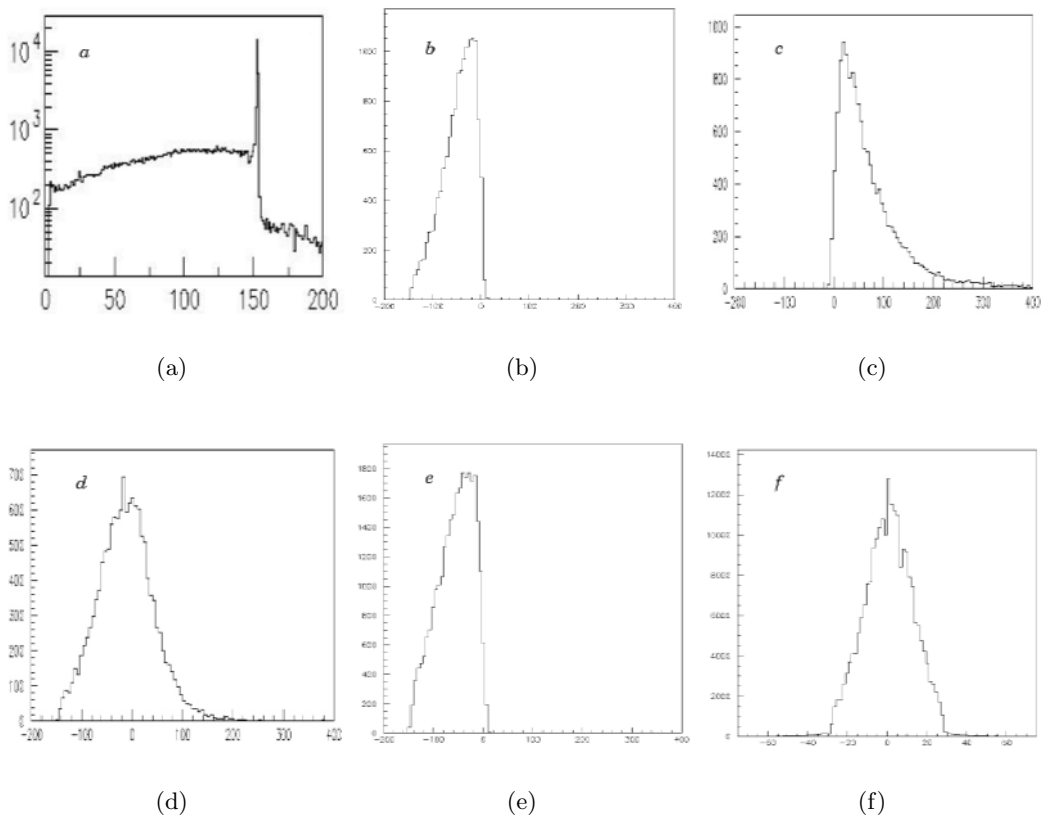


Fig. 5. Triple coincidence TDC data. a) Typical TDC spectrum showing the spike associated with events where the PMT under consideration, P_0 , defines the timing of the trigger; b) TDC spectrum of the other PMT in the tank to which P_0 belongs; c) TDC spectrum of the latest PMT; d) TDC spectrum of the earlier PMT in the tank containing the latest PMT shown in c); e) TDC spectrum of the two PMTs of the third tank; f) Time difference between the TDC channels of the two PMT's of the same tank, with an rms of 12 ns.

coincidence rate twice as large as the latter. The uncertainties on the tank times have been evaluated for each threshold and for each tank separately.

IV. A SIMPLE MODEL

The extreme simplicity of the detector prevents making accurate measurements of the shower parameters such as multiplicity, lateral distribution function, energy, etc. Yet, a very simple model allows for some qualitative description of their main features.

We recall that extensive air showers such as those detected here result from the interaction with atmosphere of primary cosmic rays, mostly protons but also heavier nuclei [3]. Their energy must exceed 17 GeV, the rigidity cut off in Hanoi associated with the Earth

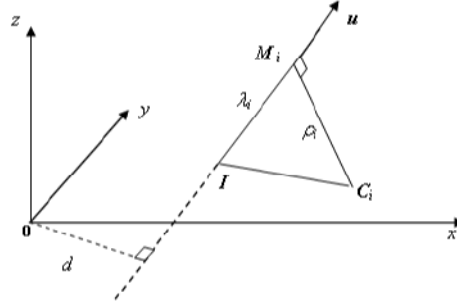


Fig. 6. Definition of the parameters used to describe a shower. The shower axis (unit vector \mathbf{u}) impacts on the roof in $\mathbf{I}(x_{imp}, y_{imp}, z_{imp})$ and a counter $\mathbf{C}_i(x_i, y_i, z_i)$ detects a signal at time $t_i = -\lambda_i$ ($c = 1$). The distance of the shower axis to the origin is d and to \mathbf{C}_i is ρ_i .

magnetic field [4]. Their differential flux decreases with energy as $0.1(\frac{E(\text{GeV})}{100})^{-2.7} \text{m}^{-2} \text{s}^{-1} \text{sr}^{-1} \text{GeV}^{-1}$. Therefore, their mean energy barely exceeds 40 GeV. For a detector having an acceptance of $22 \text{ m}^2 \text{sr}$ for triple coincidences, which is approximately the case here, the integrated flux above rigidity cut off, is therefore 2.6 kHz. However, most of the showers induced by such primaries barely reach ground – apart for the muonic component – and cannot trigger the detector. Hence studies of extensive air showers in the GeV to TeV range require high altitude observatories – or even better direct detection of the primaries from space. As Ha Noi is at sea level, vertical showers have to survive 1 kg/cm^2 of atmosphere, namely some 11 interaction lengths, to have a chance to give a trigger. But showers of such energies reach their maximum after only five interaction lengths and are well in the tail when they reach ground. The situation is much worse for inclined showers, for which the thickness of atmosphere traversed increases as $1/\cos\theta$. We expect therefore that the showers that trigger the detector will be nearly vertical and that only a very small fraction of the primary 2.6 kHz rate will have sufficient particle density on ground to give a trigger. Moreover, as the particle density increases in approximate proportion to energy (while the shower length increases only logarithmically with energy) higher energy showers will be more likely to give a trigger, the detected differential flux decreasing only as $E^{-1.7}$. We expect therefore that typical energies of the detected showers will be some factor above the mean energy of 40 GeV mentioned earlier, in the hundred to few hundred GeV region.

The shower model used here describes showers in terms of only three parameters: their solid angle Ω_0 around the vertical, their multiplicity m_0 and the radius ρ_0 of their lateral distribution function. More precisely, the solid angle $\Omega = 2\pi(1 - \cos\theta)$ is taken between 0 and 2π with a Gaussian distribution of the form $\exp(-0.5(\Omega/\Omega_0)^2)$; the multiplicity m is taken with a Poisson distribution of mean m_0 ; and the particle density in a plane normal to the shower axis is taken exponential, of the form $(m/(2\pi\rho_0^2))\exp(-\rho/\rho_0)$, ρ being the distance to the shower axis. The cross section offered by the small tanks to the shower front is easily calculated and found nearly constant, between 1.5 and 3 m^2 .

The probability for a tank to be hit by at least one particle is $1 - \exp(-w)$ where w is the average number of particles hitting the tank as provided by the model. However, the probability for the tank to give a signal is obtained from the same expression after application on w of a 35% Gaussian smearing and of a cut at 0.04 particles corresponding to the 2 ADC channels threshold. The total charge collected in the small tanks increases from 8 to 11 particles when the threshold increases from 2 to 18 ADC channels. In order for the model to reproduce these charge distributions, the approximation of a Poisson multiplicity distribution must be abandoned and good fits have been obtained by using much broader multiplicity distributions. However, a reliable quantitative comparison would need to account for the response of the counters to a given particle, which is well beyond the scope of the present study. The effective number of shower particles hitting the three tanks, 8 on average, obtained from the comparison between the simulation and the data, has only a meaning within the framework of the model and its precise relation to the real number of particles of different kinds is not simple.

The parameters of the model are adjusted to fit the data (Fig. 7). The angular distribution gives Ω_0 while m_0 and ρ_0 are obtained from the ratio between double and triple coincidences, R_3 , and from the fraction of double coincidences of tanks 1 and 2, R_2 , using model predictions.

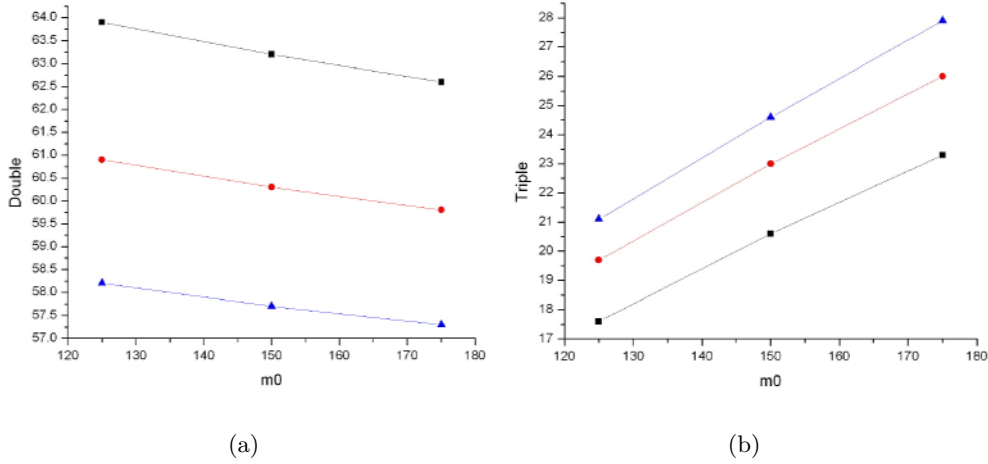


Fig. 7. The dependence on m_0 of the coincidence ratios (%) R_2 (a) and R_3 (b) defined in the text is shown for three different values of ρ_0 (200, 225 and 250 cm).

We find $\Omega_0 = 0.8 \pm 0.1$ sr, $m_0 = 151 \pm 25$ and $\rho_0 = 218 \pm 30$ cm. The predicted and measured Ω distributions are compared in Fig. 8. Here $\Omega = 2\pi(1 - \cos\theta)$ is calculated from $\cos\theta = \sqrt{1 - \alpha^2 - \beta^2}$ using (5).

The model allows for an evaluation of the detector acceptance. After integration over solid angle, it amounts to 100 m^2 and 22 m^2 for showers giving a double coincidence and showers giving a triple coincidence respectively. From the measured triple coincidence rate, 0.098 Hz, well below the integrated primary rate of 2.6 kHz, we infer therefore an

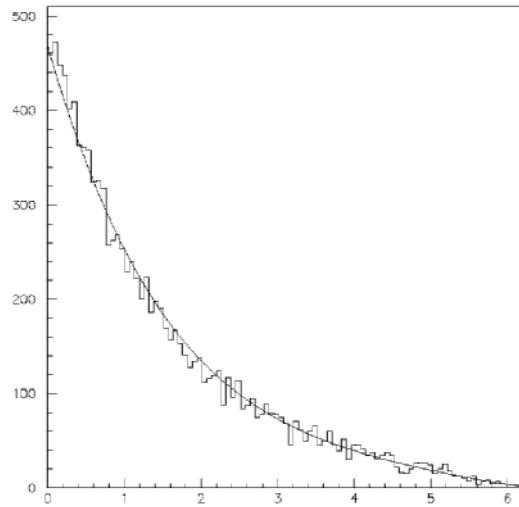


Fig. 8. The measured Ω distribution (histogram) is compared to the model prediction (curve) using a Gaussian form having $\Omega_0 = 0.8$ sr.

integrated flux of $4.5 \cdot 10^{-3} \text{ m}^{-2}\text{s}^{-1}$. For the integrated primary rate to reach such a low value, the energy threshold would have to be as high as 6.8 TeV. However, as previously discussed, the showers that trigger the detector are expected to have energies well above the 17 GeV rigidity cut off but well below this 6.8 TeV upper limit: under the assumption that the probability for a shower to trigger increases in proportion with its energy, the showers which give a triple coincidence are found to have typical energies in the 200 GeV range, an energy where the primary rate is still a factor 400 above the measured rate. The measured single tank rates are in the 100 Hz range while the contribution of showers described by the model is only at the 1 Hz level. This is not surprising: it is much easier for a shower tail to trigger a single tank than two tanks separated by a distance. In particular, muons contribute a flux [4] of $200 \text{ m}^{-2}\text{s}^{-1}$, implying that the probability for a single muon hitting a tank to give a signal above threshold is in the range of 20%.

V. RESPONSE OF THE MAIN COUNTER

On average, 10.6 particles are expected by the model to hit the main counter for triple coincidences in the small counters. This means that each triple coincidence trigger should be associated with a signal in the main counter. This prediction is corroborated by the data as illustrated in Fig. 9, providing evidence for the fact that the trigger is perfectly doing the job for which it was designed. The conversion factor from ADC channels to particles in the main tank is found to be 8.6 channels per particle from the data using a 2 ADC channel cut on the small counters. Using this factor, when the ADC cut applied to the small counter charges is increased to 10 and 18 ADC channels, the mean charge collected in the main tank increases to 12.5 and 14.6 particles respectively. This is in qualitative agreement with the values predicted by the model, 12.2 and 13.4 particles respectively. As previously discussed, a better quantitative agreement would require a

broader multiplicity distribution than the Poisson distribution used in the model in order to reproduce the charge distributions observed in the small counters. However, this is beyond the scope of the present study which concentrates on the performance of the trigger rather than on that of the main counter.

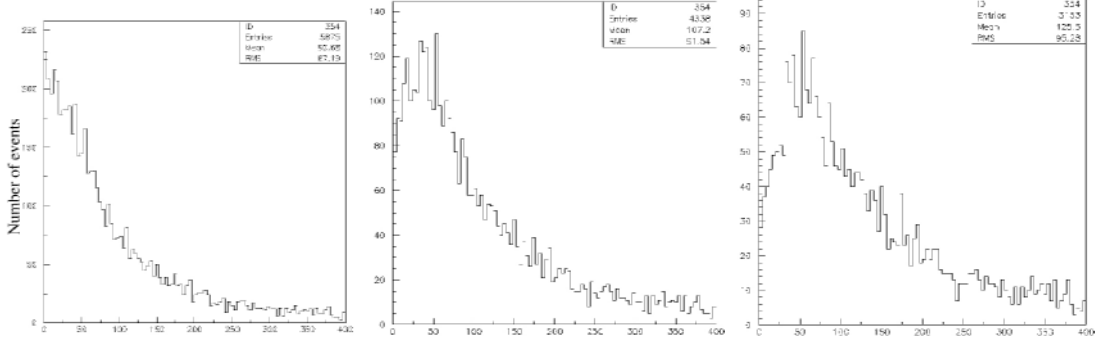


Fig. 9. Distributions of charge (ADC channels) collected in the main counter, averaged over the three PMTs, for triple coincidences of the small tanks using cuts at 2, 10 and 18 ADC channels respectively (from left to right).

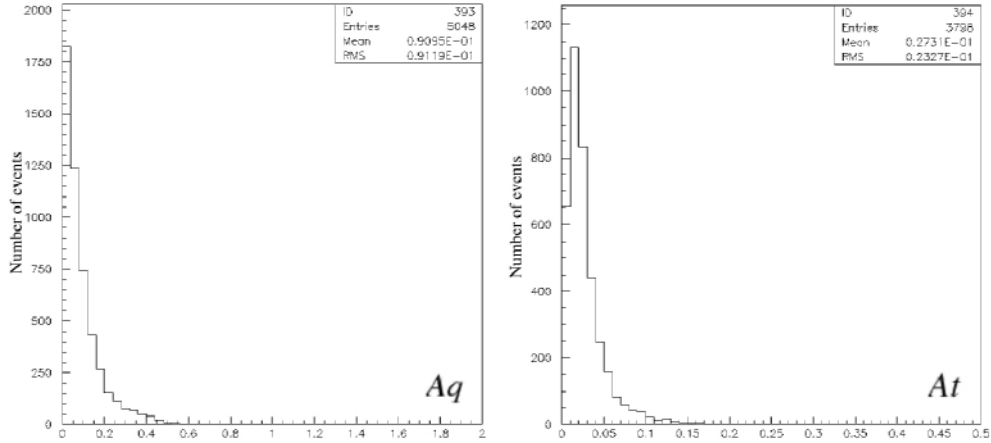


Fig. 10. Distribution of the charge and time asymmetries measured in the main counter.

Strong correlations are now observed between the charges and times measured by each of the three PMT's of the main counter. This is illustrated in Fig. 10 which displays the distributions of the asymmetries defined as $A_q = \sqrt{\sum q_i^2} / \langle q_i \rangle$ and $A_t = \sqrt{\sum t_i^2} / \langle t_i \rangle$ where q_i and t_i are the charge and time measurements obtained from each of the three PMT's. On average, the charge asymmetry is only 9% while the time asymmetry, 2.7%, corresponds to 5.6 ns. Even in the case of a perfect optical quality of water and tank walls, the Cherenkov light which reaches the PMTs photocathodes in the first 25 ns or so has no time to be randomised by the successive diffusions and is asymmetrically distributed between the three PMTs [5]. The contribution of the light

absorption in water and in wall diffusions is therefore significantly smaller than the asymmetries measured here. This result provides strong evidence that the refurbishing of the counter has been successful.

VI. CONCLUSIONS

In spite of the extreme simplicity of the detectors used as a trigger, a number of conclusions have been reached concerning its characteristics and the configuration of the showers on which it triggers:

- The triple coincidence trigger rate is 0.1 Hz. The acceptance of the detector for this trigger is of the order of 22 m². The corresponding flux of showers is 4.5 10³m⁻²s⁻¹, a factor 2 10⁴ lower than the integrated primary flux.

- At the price of a lower trigger rate it is possible to improve the accuracy of the time measurements by raising the single tank charge thresholds. A 15% improvement costs a factor 2 in rate (going from 2 to 18 ADC channels).

- The trigger selects showers within a mean solid angle of 0.64 sr around the vertical, having energies in the 200 GeV range and an effective particle density of 1 m⁻² in the region of the main counter.

The availability of such a trigger opens the door to detailed studies of the response of the main counter to low energy extensive air showers.

ACKNOWLEDGEMENTS

We are indebted to CERN, RIKEN, the World Laboratory, the EU-Asia link program, the French CNRS and the Rencontres du Vietnam for invaluable material and financial contributions. We deeply acknowledge major support from the basic research program of the Ministry of Science and Technology of Vietnam. We are particularly grateful to the Pierre Auger Collaboration for their constant interest and support in the development of our group.

REFERENCES

- [1] The Auger Collaboration, J. Abraham *et al.*, *Nucl. Inst. Meth.* **A523** (2004) 50; A. A. Watson, *Highlights from the Pierre Auger Observatory*, presented at the 30th ICRC, Merida, Mexico, 2007.
- [2] P.N. Diep *et al.*, *Proc. VIth Renc. Vietnam*, 2006, to be published; P. T. T. Nhung, *Performance Studies of Water Cherenkov Counters*, Master thesis, Vietnam University of Sciences, Hanoi, 2006; P. N. Dong, *The Cherenkov Counters of the VATLY Laboratory*, Master thesis, Hanoi University of Technology, 2006; N.T. Thao, *The Detection of Extensive Air Showers in Hanoi*, Master thesis, Hanoi University of Sciences, Hanoi, 2007.
- [3] A.M. Hillas, *Ann. Rev. Astron. and Astrophys.*, **22** (1984) 425; M. Nagano and A.A. Watson, *Rev. Mod. Phys.*, **72** (2000) 689.
- [4] P. N. Diep *et al.*, *Comm. in Phys.*, **15** (2005) 55.
- [5] D. T. The, *Optical Properties of a Cherenkov Counter*, Hanoi National University of Education, Hanoi, 2007.

Received 31 May 2007.

